ICAM
10th International Congress for Applied Mineralogy
Trondheim 2011

UNDERSTANDING MICRO-ENVIRONMENT DEVELOPMENT IN MINE TAILINGS USING MLA AND IMAGE ANALYSIS

Mostafa Redwan[1,2], Dieter Rammlmair[1*]

[1]BGR, Sub-Department 1.2 Resource Geology, Polar Geology, Working Group Mineral Residues, Stilleweg 2, D-30655 Hannover, Germany

[2]Geology department, Sohag Faculty of Science, Sohag University, Sohag, Egypt

Abstract

In the course of ore mineral treatment large amounts of mineral residues will be deposited in tailings dams. The spilled material might contain some amount of valuable as well as hazardous material. The spilling process generates vertical and lateral mineral and grain size fractionation. Mine tailings therefore show distinct chemical and mineralogical pattern along the spilling path and across the same, completely different from the initially spilled material. Spilling pulses and migrating spilling points cause local enrichment of individual phases such as sulfides, micas, etc. After deposition these finely laminated mine tailings are exposed to alteration. Alteration is not homogeneous. The variable degree of water saturation and the position of the oxidation front are basically due to inclination of lamina, and to changes in grain size along the transport path. But even at the relatively coarse rim intercalated fine grained lamina change the hydraulic properties, creating capillary barriers, lamina with enhanced water retention capacity etc. Alteration occurs in microenvironments at the boundaries of lamina contrasting in grain size, porosity, saturation, mineralogy, redox, pH, and chemistry. The dissolution, oxidation, and hydration of minerals cause a loss and gain of volume, , generating micro-porosity within minerals and clogging pores at different positions respectively. In this paper, optical microscopy, automated mineralogy using a FEI-ESEM based mineral liberation analyser (MLA) system on dry polished thin sections, and image analysis are combined to define characteristic features such as porosity, primary and secondary phases, grain size, and mineral assemblages for individual lamina to highlight boundaries of contrasting features being responsible for the development of micro-hardpans. The aim is to develop new strategies for auto-remediation, and to localize zones of anomalous enrichment of potentially valuable metals.

Keywords: mine tailings, lamination, micro environment, MLA, mineralogy

1 INTRODUCTION

Mining industry generates enormous amounts of mineral residues such as mine tailings, covering huge areas and being responsible for locally extreme environmental problems due to wind and water erosions, dam failure, or mine drainage. Part of these depositories might contain highly valuable minerals, either in formerly sub-economic amounts or not yet recognized as such. Due to the increasing demand for metals for advanced technologies, sophisticated strategies are needed to localize and extract valuable and contaminating minerals,

* Correspondence to: rammlmair@bgr.de

Maarten A. T. M. Broekmans (ed.), *Proceedings of the 10th International Congress for Applied Mineralogy (ICAM)*, DOI: 10.1007/978-3-642-27682-8_70,

and even to use the residues as building materials or to deposit them according to highest ecological standards. This requires fast and cheap methods to characterize residues according to their economic and ecologic potential, to optimize and modify mineral treatment processes, and to develop depositional strategies able to prevent or reduce rock drainage, wind and water erosion, and area consumption.

Weathering processes in tailings are responsible for substantial changes of the external and internal structure of the heap. This is basically due to changes in mineralogy, which influence the hydraulic properties. Either reduction of permeability due to clogging of pores or higher porosities due to selective leaching can be observed [1]. Graupner et al. [2] found that to form hardpan/cemented layers in tailings, premises such as critical accumulation of reactive phases in thin layers, intercalation of silt and sand layers, small inclination of the layers, perhaps microbial activity to promote dissolution and precipitation, and climatic support are of major importance. Hardpans, even extremely thin (few millimetres), but eventually multiply repeated, might show a strong influence on water migration through a heap, eventually drying out the core of the heap itself. On the other hand, hardpans and cemented layers might be responsible for economic enrichment of metals. To decipher the processes taking place and the progress of the alteration of a sedimentary system where each lamina displays an almost unique composition, combinations of analytical methods have to be applied. Besides bulk methods, even for minute subsamples spatially resolving 2D and even 3D methods have to be taken into consideration. The spatially resolving methods provide quantification of mineralogical compounds, on their relationship, intergrowth, ratios, besides diameters, size, surface irregularities, shape, roundness orientation, distance between features and its numbers, and its textural relationships, etc.

The work presented here focuses on mine tailings, and the structural reorganization of the deposition induced texture by alteration processes taking place. Our main objectives in this study is to show, how automated mineralogy (MLA) can be used as a valuable tool to characterize microenvironments

2 MATERIALS AND METHODS

2.1 General

The Davidschacht tailings impoundment north-east of the town of Freiberg, Germany, was used from 1951 to 1964 for the discharge of mine tailings from mineral treatment of poly-metallic sulfide ore of Late Variscan age. The two ore paragenesis consisted of sulfides and quartz with some carbonates, and sulfides, carbonates and/or barite [3], respectively. The host rock in the Freiberg district includes gneisses, mica-schists, and amphibolites. The height of the impoundment reaches 60 m, and covers a surface area of about 7.5 ha. An artificial dam was built to the N and E and on the western side coarser materials were used as wall [4] . The western flank consists of three major 5-m steps each with a 5-m wide flat top to provide access to the spilling equipment. Each of the steps is subdivided into five 1-m substeps. The substeps were manipulated by hand to form barriers. The material is throughout laminated and displays numerous hardpans and cemented layers alternating with less altered material, only exposed in excavated areas. These intercalations point towards changes in the techniques, for example, gravity to flotation separation. Finally, the impoundment was partly covered from the top with coarse sand and topsoil (about: 0–0.2-m thickness) and plants.

2.2 Materials

The sampling was performed along excavated trenches at the western flank of the tailings impoundments. Samples were collected in the cm scale for individual layers in plastic bags or in small plexiglass boxes to keep the original lamination. Each hardpan sample was first cut into two parts, one crushed homogenous and pulverized to grain sizes less than 5 μm with RS 200 instrument with agate milling

set (Retsch GmbH), for standard XRD and XRF analysis. The other part was mapped using EDXRF-microscope for 2D-element distribution in 100-m or 200-μm steps. From the overview obtained, areas of interest were selected for polished thin section for further detailed investigation. The preparation of polished thin sections was performed in a special way to prevent further oxidation and preferential leaching of some of the phases. Cutting, grinding, and polishing was done under completely dry conditions. Then the polished sections were scanned by a slide scanner with // and X polarisations, and investigated by optical microscopy (penetrated and reflected light). FEI Quanta 600 FEG ESEM (Environmental SEM) was used for the detailed characterization and identifications of primary phases and secondary crystalline and amorphous phases as well as for textural relationship under low vacuum conditions. Quantification was done by applying the MLA software package.

EDXRF microscope

The ITRAX X-ray Microscope (Cox Analytical Systems AB, Sweden) is used for multi-elemental mapping of vertical or horizontal polished slices of sizes up to 20 × 30 cm, which mounted on an *xyz*-stage. It is based on a Rich. Seifert & Co. ISO-DEBEYEFLEX 3003 HV-Generator and a 3 kW, 60kV long fine focus Philips XRD Mo tube Type PW 2275/20. However, the beam is focused by a glass mono-capillary to 100-μm diameter. The energy dispersive RÖNTEC XFlash Si(Li) detector of 139-eV resolution with an evacuated nozzle mounted in 45° between detector and sample [5]. Elemental mapping was performed at 45kV, 30 mA, .5 s, 100-μm step size with spectra evaluation by preadjusted Qspec 6.5 Software. The obtained maps were changed by MapView in to *.jpg images (COX Analytical Systems AB, Sweden) for further manipulation by image analysis.

Optical microscopy, mineral liberation analyser (MLA) and image analysis software packages

Using Leica DM4500 P microscope with Leica DFC camera (Leica Microsystems GmbH, Germany), polished thin sections were investigated. Then the samples were subsequently studied by using an Environmental Scanning Electron Microscope, type FEI Quanta 600 FEG ESEM coupled with EDX detector (Apollo XL from Ametek Inc.) for detailed characterization, identification, and quantification of primary and secondary crystalline and amorphous phases as well as for textural relationships. The investigation was conducted by applying MLA software package in the XBSE (Extended BSE Liberation Analysis) mode. BSE images are collected, particulated to differentiate pores, grains, and to remove subgrain. They are then presegmentated to remove holes and cracks, and finally within grains the grey value contrasting between minerals are localized. In the next step, an EDX Spectrum is acquainted from each identified grain and compared with a prepared database.

Due to the fine grain size, the pore filling gels and alteration patterns, the GXMAP (Ford Analysis or Grain based X-ray Mapping) mode was used. This method collects X-ray spectra for the mineral grain by using a closely spaced grid system [6]. While BSE image mosaics were obtained for the whole thin sections, the MLA was acquainted from selected areas only. Both were evaluated by image analysis. From BSE images better statistics for few phases, porosity, grain size, sulfides could be obtained, from MLA individual phase distribution, grain size etc. Information of single lamina was extracted by defining regions of interest (ROI). From MLA images binary images of individual phases were extracted and evaluated along the profile for grain size and volume at any point in the section profile. 2D was reduced to a 1D grayscale profile and subsequently plotted using excel and panplot (from Pangea). In the second step, zones of contrasting features such as grain size, and clogging of pores were used to identify ROI's. For each region of interest porosity and all minerals were evaluated for parameters such as size, area, perimeter, diameter etc.

3 RESULTS

The bulk XRD analysis of the samples gave quartz as the main constituent, then muscovite-illite, chlorite, gypsum, and jarosite. The grain sizes are mainly in the fine sand range (about 60%), the rest is distributed in the very fine and medium sands.

The polished thin sections were scanned with a slide scanner under parallel (Figure 1b) and crossed polars to obtain a textural overview. All sections displayed fine lamination of alternating fine and coarse grained lamina. Some of the layers appeared to be graded according to grain size distribution and showed local enrichment of heavy minerals and/or sulfides. From microscope observation, optical slide scanning, and EDXRF element mapping (Figure 1c and d) and SOM (self-organized mapping, Figure 1e and f) evaluation (by A. Bahr, BGR), the mineralogy basically consisted of primary phases such as quartz, plagioclase, potassic feldspar, amphibole, biotite, muscovite, some accessories such as calcite, dolomite, ankerite, zircon, pyrite, arsenopyrite, chalcopyrite, cassiterite, and others. Metamorphic predepositional phases are actinolite, chlorites, phengite, illite, albite etc. whereas vermiculite, clays, most of the Fe-hydroxides, amorphous gels, gypsum, jarosite, and scorodite are post-depositional weathering products. Alteration of sulfides and silicates after deposition was not homogeneous. Besides completely unaltered lamina, all stages of replacement and alteration were observed, ranging from incipient to total alteration (Figure 2a), with the formation of sulfates and gel of different compositions (Figure 2b). Individual laminas were totally or partially altered. Some lamina packages exhibited dark brown rims, partly irregular, partly interrupted by pale yellow finger zones reaching deeper levels. Zoning with outer Fe-rich rim surrounding a central As–Fe-rich laminated zone, has also been recognized. These Fe and As enriched zones relate basically due to a number of crystalline and amorphous secondary products showing scattered distribution, or local enrichment of some of the primary phases or display dense layers where pores are almost quantitatively locked. Common secondary phases are various Fe-oxy/hydroxides or hydroxysulfates such as hematite, goethite, limonite, amorphous, gypsum, scorodite, jarosite, and a number of gels of different colour and composition. The primary textural premises were expected to control at least some of the alteration features. Therefore, investigation of the relationship of the alteration and the primary texture was pattern of special interest.

An optical identification of secondary phases is highly problematic, since some of them are really small and often stained by other secondary phases.By implementing MLA techniques even small phases could be chemically characterized along a central position in the thin section approximately one mm wide and 4-cm long area, perpendicular to the lamination, a quantification (area-%) of all phases, identified by means of the newly generated BSE-grey value and EDX-spectra based MLA database. Individual colours were attributed to individual phases and minerals, and presented in a distribution map. A number of lamina could be identified showing distinct features (Figure 3), such as grain size grading of quartz and feldspars, enriched layers of mica and amphiboles, of sulfides, of accessory minerals. Porosity shows some remarkable changes. There are zones where almost all pores are clogged by secondary phases, dominantly by gels of varying chemical composition.

Looking to the different minerals in detail we can extract an enormous amount of data by MLA due to the extreme details visualized on the µm-scale. The variation of mineral assemblages at this scale makes it extremely difficult to extract the dominant assemblages, responsible for this type of alteration and reorganization. Within the individual lamina the change of porosity is a prominent feature. Image analysis was used to pixelwise (2µm) erode pores. Zones with dominant gel clogging close all passageways with the first (drying cracks) or second step of erosion. Remnant porosity refers to larger isolated non communicating pores. Whereas in sections of coarser grains 3 to 7 steps of erosion are needed to isolate pores. Since the gel might contain high amounts of water, a significant volumetric change due to oxidation, carbonation, and hydration is expected to take place. We assume that most of the material used for the gels is from the

immediate surroundings with some removal of material like Fe^{2+} and As^{3+} in the early state of incipient oxidation and saturation. All the amorphous As–Fe precipitates showed a desiccation cracks texture. The gels show a number of generations chemically different. Itis worthwhile to note that the early gel layers coat all phases within a layer of relatively constant thickness of several μm whilst later gels clog the pores. Some layers are heavily altered showing almost no reactive primary phases. Generally, in case of gel zoning, the outer rims are high in water content, arsenic, and somewhat iron, while the inner rims are high in silica, potassium, and sulfur content.

In the thin section under study of hardpan sample (Figure 3), the porosity turns out to be quite variable. For example, at two distinct zones, the pores are almost filled by gels, sulfates or K-jarosite. At depth from −056.6 to −0.59 cm, the porosity reached average 13.4 area-%, due to the precipitation of gels (average 46.83 area-%,) and scorodite (average 2.47 area-%,). At depth from −0.64 to −0.66, the porosity reached average 18.9 area-%, due to the precipitation of gels (average 38.75 area-%), gypsum (average 10.9 area-%), and scorodite (average 1.479 area-%), (Figure 3). Also, at depth from −0.81 to −1.08, the porosity reached 21.78 due to the precipitation of gels (average 21.76 area-%), gypsum (average 12.75 area-%) and jarosite (average 1.26 area-%). Gypsum, showed a patchy distribution throughout the section. It increased with sulfides near the surface (between −0.6 and −1.0 cm,). Most scorodite grains characterized by dispersed spherules, found in areas where a higher porosity is available in the upper surface, accompanied with sulfides at −0.4 to −0.9 cm (average content 2.7 area-%). in the vicinity of the amorphous gel layers (i.e. in the transition zone between amorphous gel layers and the underlain high porous areas), from which the scorodite crystallized. Quartz and chlorite distributed along the whole section and decreased in areas of higher porosity. Barite and accessory minerals showed two distinct peaks around −0.7 and −1.35 cm.

4 DISCUSSION

Hardpan samples from Davidschacht mine tailings impoundment in Freiberg, Germany, have been investigated within a micrometre–-millimetre scale in detail, in order to visualize the different stages of alteration and the development of hardpan layers. The depositional dynamics is documented by alternating graded bedding for individual phases, generating characteristic transitions from fine grains toward the top to coarse-grained toward the bottom with localization of sulfides and other heavy minerals in certain lamina. The alteration of sulfides showed different stages depending on the availability of oxygen and water at each distance from the grain surface. The precipitation of amorphous As–Fe (with desiccation crack texture), and the presence of gels of several generations different in chemistry are related to the periodic acidic drainage water and re-precipitated due to As co-precipitation with and/or adsorbed onto iron oxides, resulting in the formation of cements with varying levels of As. This phenomenon also recorded by Courtin-Nomade et al. [7] at the surface of metalliferous mine tailings in France and Ahn et al. [8] at the tailings pile of the Nakdong mine in Korea. As low pH values resulted from sulfides oxidation, the aluminosilicates became unstable and affected by dissolution then released the alkali ion to the surrounding [9]. The localization of most K-jarosite in certain horizons correspond to areas of higher concentration of micas, which take the required alkali ion for its precipitation, whereas the gypsum which showed a patchy distribution throughout the section, especially, in the upper surface layers, may be due to the increase percent of SO_4 in the solution in combination of Ca enough for its precipitation. Scorodite which formed under low pH environment [10] as a result of arsenopyrite oxidation [11] was found in the upper surface layers with altered sulfides layers.

5 CONCLUSIONS

The use of MLA for quantitative mineralogy in laminated tailings is a highly valuable approach to decipher grain size distribution of individual minerals caused by the sedimentation process and to elucidate the systematic coincidence of mineralogy and textural premises generating local enrichment of primary reactive phases in distinct zones of elevated hydraulic contrast such as very fine grained layers able to hold water for a prolonged time period, and coarser portions providing access of air or fresh, oxygen saturated water to the mineral phases. Oxidation, dissolution, short transport, and precipitation are promoted. Precipitation of secondary phases and gels is due to physicochemical gradients of pH, redox, or temperature, which has the major influence on porosity reduction at distinct zones. MLA is the optimal tool to provide sub-microscopic mineralogical information for reactive transport modelling at pore scale.

6 REFERENCES

[1] Rammlmair, D (2002): Hardpan formation on mining residuals. In: Merkel, B, Planer-Friedrich, B, and Wolkersdorfer, C (editors). Uranium in the Aquatic Environment. Proc. Int. Conf. Uranium Mining and Hydrogeology III and International Mine Water Assocation Symposium, TU Bergakademie Freiberg, Germany, 15–21 Sept. :173–182.

[2] Graupner, T, Kassahun, A, Rammlmair, D, Meima, JA, Kock, D, Furche, M, Fiege, A, Schippers, A, and Melcher, F (2007): Formation of sequences of cemented layers and hardpans within sulfide-bearing mine tailings (mine district Freiberg, Germany). Applied Geochemistry (22):2486–2508.

[3] Tichomirowa, M, Pelkner, S, Junghans, M, and Haubrich, F (2002): Sulfide oxidation at the polymetallic sulfide deposit Freiberg (Germany) and consequences for heavy metal mobilization. In: Schulz, HD, and Hadeler, A (editors): Geohemical processes in soil and groundwater measurement–Modelling– Upscaling, GeoProc 2002, Wiley–VCH, Weinheim : 356–379.

[4] G.E.O.S. (1993): Freiberg Ingenieurgesellschaft mbH. Kurzbericht zur Gefährdungsbschätzung der Davidschcht-Spülhalde, Freiberg, März1993.

[5] Rammlmair, D, Wilke, M, Rickers, K, Schwarzer, RA, Möller, A, and Wittenberg, A (2006): Geology, mining, metallurgy. In: Beckhoff, B, Kanngießer, B,. Langhoff, N, and Wedell, R (editors): Handbook of Practical X-Ray Fluorescence Analysis., Springer, Heidelberg. Chapter (5.6): 640–687.

[6] Fandrich, R., Gu, Y, Burrows, D, and Moeller, K (2007): Modern SEM-based mineral liberation analysis. International Journal of Mineral Processing (84):310–320.

[7] Courtin-Nomade, A, Brila, H, Neela , C, and Lenain, J-F (2003): Arsenic in iron cements developed within tailings of a former metalliferous mine—Enguialès, Aveyron, France. Applied Geochemistry (18): 395–408.

[8] Ahn, JS, Park, YS, Kim, J-Y, and Kim, K-W (2005): Mineralogical and geochemical characterization of arsenic in an abandoned mine tailings of Korea. Environmental Geochemistry and Health (27): 147–157.

[9] Dutrizac, JE, and Jambor, JL (2000): Jarosites and their application in hydrometallurgy. In: Alpers, CN, Jambor, JL, and Nordstrom, DK (editors): Sulfate Minerals: Crystallography, Geochemistry, and Environmental Significance. Reviews in Mineralogy and Geochemistry, Vol. 40: 405–452.

[10] Haffert, L, and Craw, D (2008): Mineralogical controls on environmental mobility of arsenic from historic mine processing residues, New Zealand. Applied Geochemistry (23):1467–1483.

[11] Dove, PM, and Rimstidt, JD (1985): The solubility and stability of scorodite, $FeAsO_4.2H_2O$. American Mineralogist (70): 838–844.

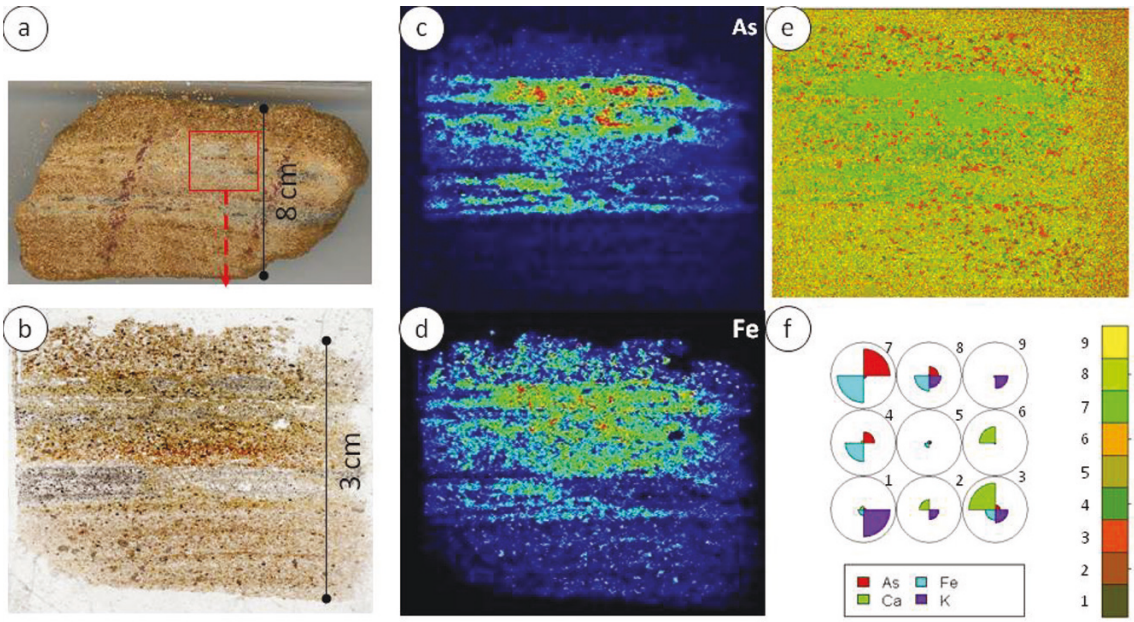

Figure 1: (a) Cut hand specimen of hardpan; (b) optical scan of dry polished section (no loss of dissolvable phases); elemental distribution maps by EDXRF microscope of (c) As and (d) Fe (100-µm steps, 0.5 s, 45kV, 30mA); (e) chemotextural information by SOM (self organized maps) based on EDXRF microscope elemental maps of As, Fe, Ca and K with (f) key for compositional classes.

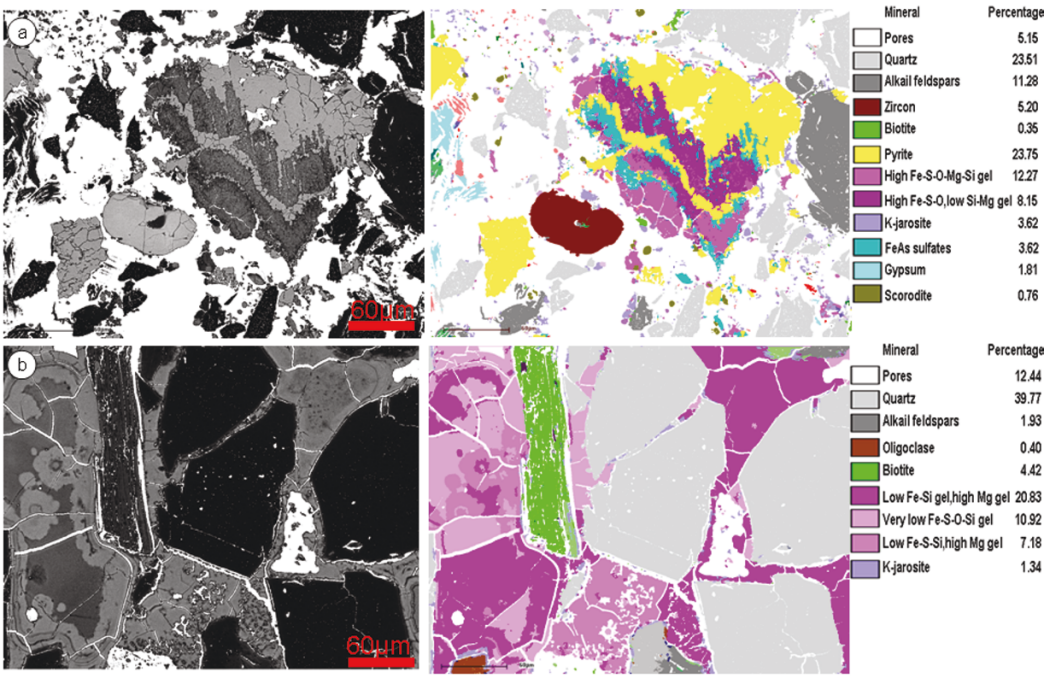

Figure 2: Detailed MLA measurement on altered pyrite crystal (a) and a collform gel (b).

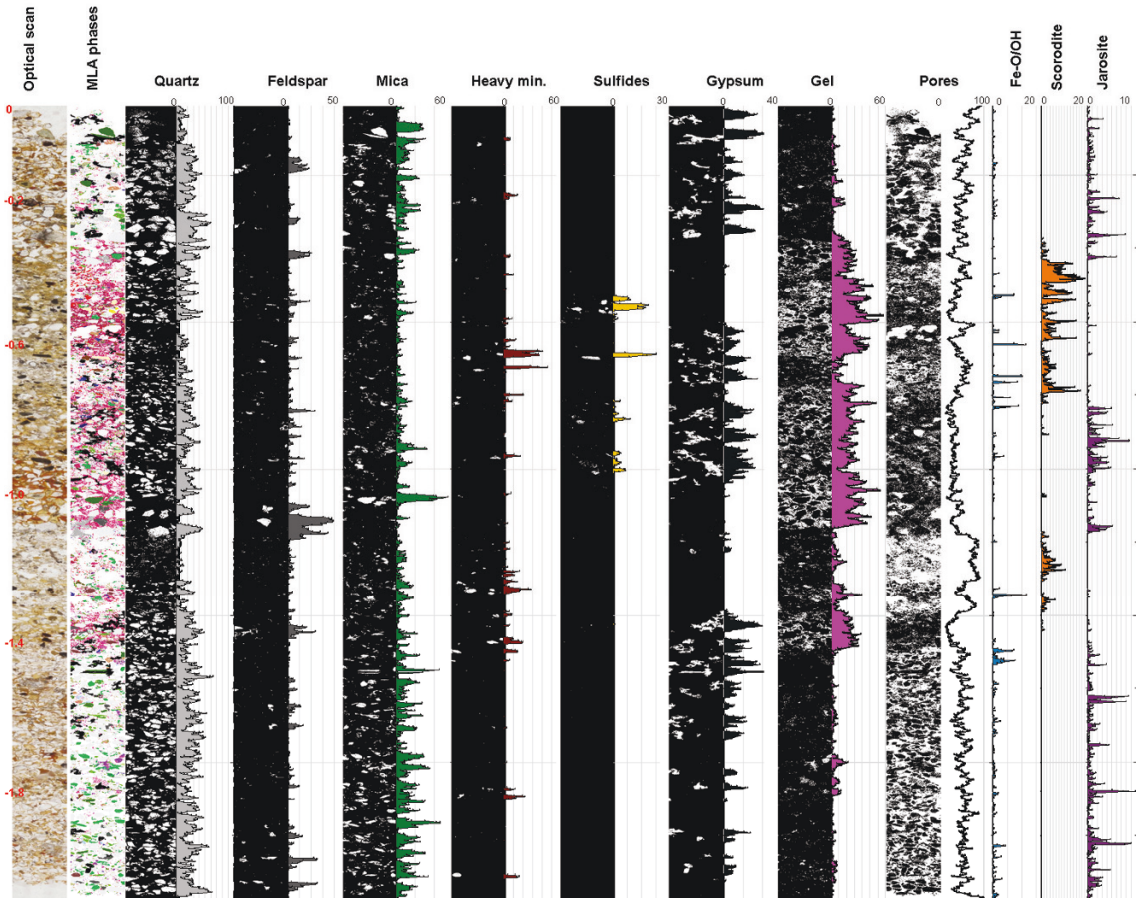

Figure 3: Assemblage of optical image (// polarisation), MLA phase map and individual phases separated and quantified by image analysis for each pixel row (= 4-µm high). The assemblage highlights the relationship of phases to porosity and clogging.